IEEE Access
Multidisciplinary ⋮ Rapid Review ⋮ Open Access Journal

Received August 23, 2019, accepted August 31, 2019, date of publication September 3, 2019, date of current version September 18, 2019.

*Digital Object Identifier 10.1109/ACCESS.2019.2939291*

# A 10-Way Power Divider Based on a Transducer and a Radial Junction Operating in the Circular $TM_{01}$ Mode

**JOSÉ R. MONTEJO-GARAI[1], JORGE A. RUIZ-CRUZ[2], (Senior Member, IEEE), AND JESÚS M. REBOLLAR[1], (Member, IEEE)**

[1]Information Processing and Telecommunications Center, Grupo de Electromagnetismo Aplicado, Universidad Politécnica de Madrid, 28040 Madrid, Spain
[2]Escuela Politécnica Superior, Universidad Autónoma de Madrid, 28049 Madrid, Spain

Corresponding author: José R. Montejo-Garai (joseramon.montejo@upm.es)

This work was supported by the Spanish Government through the Agencia Estatal de Investigacion, Fondo Europeo de Desarrollo Regional (AEI/FEDER, UE), under Grant TEC2016-76070-C3-1/2-R (ADDMATE).

**ABSTRACT** This work presents a 10-way Ku-band power divider using a mode transducer and a radial junction connected by an overmoded circular waveguide operating in the $TM_{01}$ mode. The circular symmetry of this mode has been exploited to obtain a power divider with the rectangular output ports radially distributed along the broad wall of the waveguides in *H*-plane configuration. This topology provides the same amplitude and phase for all the output ports. At the same time, a compact profile has been obtained, introducing a simple manufacturing for the two components of the divider. The first component is a mode transducer converting the $TE_{10}$ mode in the rectangular waveguide to the $TM_{01}$ mode in the circular waveguide. It is based on a novel topology providing a very high purity in the mode conversion with an attenuation for the other propagating mode, the $TE_{11c}$, higher than 60 dB. The second component is a 10-way radial junction that must work under the excitation of the $TM_{01}$, whose special features, since this mode is not the fundamental one of the circular waveguide, will be highlighted. The final design has been validated with an experimental prototype, proposing a manufacturing based on four simple parts. This has been the key to obtain an experimental prototype with specifications in the state-of-the-art. The measured efficiency is better than 96.5% in a 16.7% relative frequency bandwidth from 11 GHz to 13 GHz, with return losses better than 25 dB in the common port. The measured difference between the signals at the output ports of the prototype is $\pm 0.3$ dB for the amplitudes and $\pm 0.45°$ for the phases. A comparison of the obtained results with another divider based on the $TE_{01}$ mode shows the potential of the presented design for becoming an alternative to the more extended $TE_{01}$-based power dividers.

**INDEX TERMS** Microwave power combiner/divider, waveguide $TM_{01}$ mode transducer, mode-conversion purity, overmoded circular waveguide, radial junction.

## I. INTRODUCTION

Actual microwave systems at Ku-band are found in industrial equipment, research laboratories, or defense facilities. The applications are very diverse, involving radars for weather surveillance or traffic control, the front-end of communication transceivers or equipment for plasma science. In all these areas, the need of high-power modules is very common, with very stringent specifications of linearity and efficiency, in frequency bands that are progressively higher and wider in relative bandwidth. Devices based on vacuum technology have been commonly used in these applications [1], although solid-state technology has been under constant evolution during last decades and provides many advantages [2].

In many systems, a single unit of a solid-state power amplifier (SSPA) cannot provide the required performance with a prescribed stringent input-output linearity and high enough output power level. In this case, the combination of several sources coming from individual amplifiers is used to overcome this limitation [3], [4]. This scenario has increased the research on power dividers/combiners with a large number of ports *N* and very stringent specifications [5], [6]. One of

The associate editor coordinating the review of this manuscript and approving it for publication was Haiwen Liu.

  

the main goals in their design is to obtain a high combination efficiency, which requires that the amplitudes of the signals divided/combined in the amplification process must be controlled and kept equal in both amplitude and phase. This specification is a very important aspect of the design proposed in this work.

There are different configurations of power dividers/combiners [3], [4] such as the chain or corporate architectures, or those based on a radial arrangement of the output ports with respect to the input common port [7], [8]. The radial configuration has an intrinsic advantage based on its symmetric topology, especially for systems dealing with a large number of ports $N$, as it is the case of this work ($N = 10$) shown in Fig. 1. In this configuration all the ports are treated in the same way, since the control of the signals in both amplitude and phase is guaranteed by the field pattern of the exciting mode and the divider topology. The radial configuration can be implemented in diverse transmission media such as planar or waveguide technologies. However, when low insertion losses and high power-handling capability are needed, waveguide technology is the most suitable solution for high-power modules [9], [10].

Different type of waveguide radial combiners (or dividers, since both modes of operation are dual, and, hereafter, both terms will be used indistinctly) based on the $TE_{01}$ mode of the circular waveguide can be found in the technical literature [9]–[13]. A comparison of different designs using this $TE_{01}$ mode can be found in [9]. However, for designs based on the $TM_{01}$ circular mode, the scenario is completely different, since the number of previous contributions is scarce. In fact, the only work found by the authors dealing with a $N$-way divider based on the $TM_{01}$ mode is [14], showing a narrow band 4-way waveguide combiner centered at 14 GHz with insertion loss of 0.25 dB.

Therefore, the main goal of this work is to fill the gap in this area, designing a highly efficient power combiner based on the $TM_{01}$ circular mode, exploiting its advantages for achieving an extraordinary balance of the output signals in amplitude and phase, with low insertion and return losses, and high-power handling capability. These figures of merit will be compared with a combiner based on the $TE_{01}$ mode working at the same frequency band, showing that the presented design is a suitable alternative.

In fact, the presented configuration also provides additional degrees of freedom for arranging the ports and for simple manufacturing. In the introduced $TM_{01}$-based combiner, the output ports are placed in the so-called $H$-plane configuration, with the output rectangular waveguides distributed along their width (the "$a$" dimension) as shown in Fig. 1. This configuration guarantees that the output signals are all polarized in the same direction. However, in $TE_{01}$-based combiners, the output ports are distributed in $E$-plane along the height (the "$b$" dimension) of the output waveguides, and, two output ports placed 180° apart in the radial configuration are polarized in opposite directions. In addition, the $H$-plane configuration for the $TM_{01}$-based combiner plays a key role

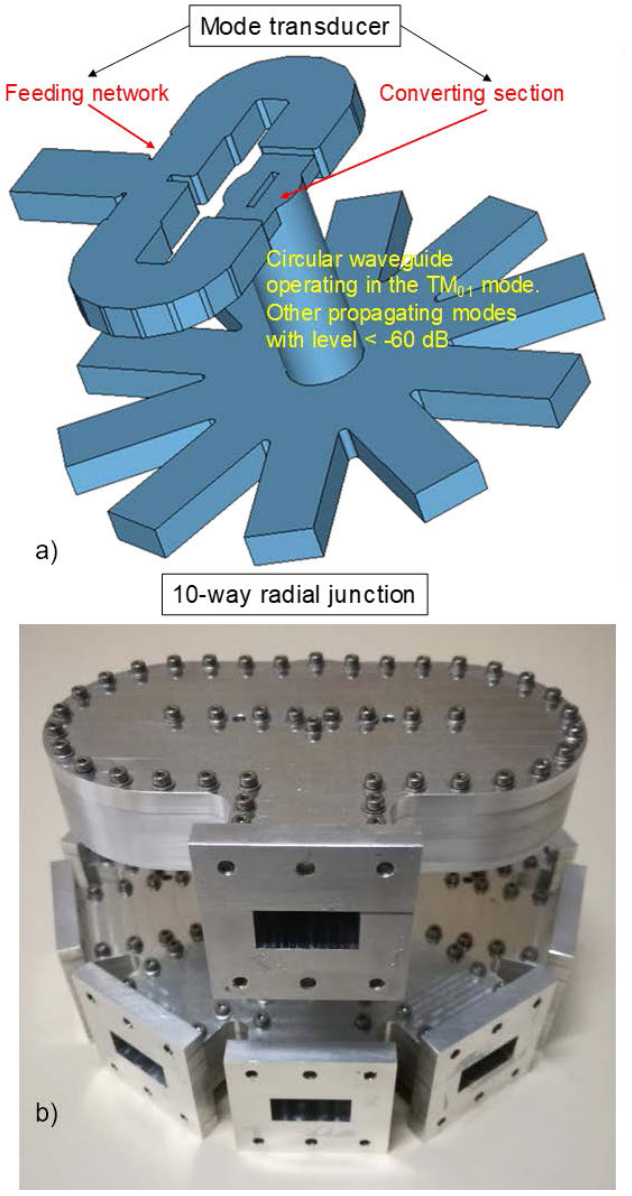


**FIGURE 1.** a) 3D view of the power divider composed of a mode transducer (between the $TE_{10}$ rectangular mode and the $TM_{01}$ circular mode), and the 10-way radial junction excited by the $TM_{01}$ (not the fundamental mode of the circular waveguide). b) Prototype manufactured in aluminum with the scheme proposed in the paper: Four simple and low-cost parts of body an cover as in $H$-plane technology.

for low cost manufacturing, since a body/cover implementation for its two main parts will be proposed, demonstrating an excellent performance.

Fig. 1(a) shows a 3D view of the power divider proposed in this work composed of two main parts: the mode transducer between the $TE_{10}$ rectangular mode and the $TM_{01}$ circular mode, and the 10-way radial junction. It is important to emphasize here that the 10-way radial junction in Fig. 1(a), although it has a radial distribution shown in other microwave structures, it is working under the excitation of the $TM_{01}$ circular waveguide mode. This leads to singular features in comparison with other junctions found in the literature, which

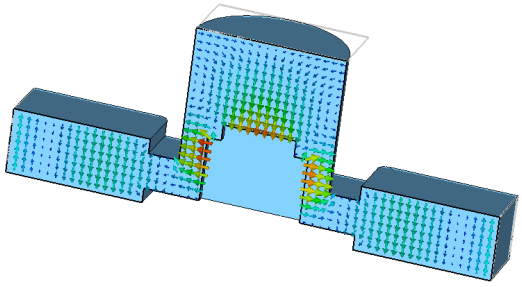

**FIGURE 2.** Converting section in Fig. 1(a) (cut at the middle of the structure showing the electric field configuration), based on a septum-type junction excited by the fundamental $TE_{10}$ mode with the same phase in both rectangular ports.

are discussed in the paper. The high purity of the $TM_{01}$ mode in the overmoded circular waveguide is preserved in the whole operation band from 11 to 13 GHz (16.7% relative bandwidth) (keeping the level of other propagating modes below −60 dB. A photo of the manufactured prototype in aluminum is shown in Fig. 1(b).

The design, manufacturing, and test of this divider is addressed in the five sections of the paper. Section II describes the design of the mode transducer composed by the converting section and the feeding network, showing the theoretical results of both elements and its complete response. Section III presents the design of the 10-way radial junction with the theoretical simulations. Experimental results of the manufactured prototype, validating the novel design, are shown in section IV. Finally, section V summarizes the contributions of this work.

## II. DESIGN OF THE MODE TRANSDUCER BETWEEN THE RECTANGULAR $TE_{10}$ MODE AND THE CIRCULAR $TM_{01}$ MODE

The transducer proposed in this work is based on a junction with three ports: two rectangular waveguides and a circular waveguide. The rectangular ports are standard WR75 waveguides. The junction is excited by means of sidewall coupling using a reduced-height waveguide. The inner part of the circular waveguide can be seen in Fig. 2, with a stepped septum to control the matching level in the converting section. When the junction is excited by two in-phase $TE_{10}$ rectangular modes, the $TM_{01}$ mode is generated at the output circular waveguide. The same figure shows the electric field in the longitudinal section of the junction, where its strength is maximum. In addition, the figure shows the actual aspect ratio of the converting section, where dimensions that could be too small for an accurate manufacturing have been intentionally avoided, improving also the power handling.

The mode transducer has been designed following the detailed procedure introduced in [15], which takes into account the excitation and the symmetries of the different parts of the transducer. Other options for this waveguide component are available in the technical literature. There are classic works and more recent contributions [16]–[19], with very diverse characteristics in the topology, bandwidth and

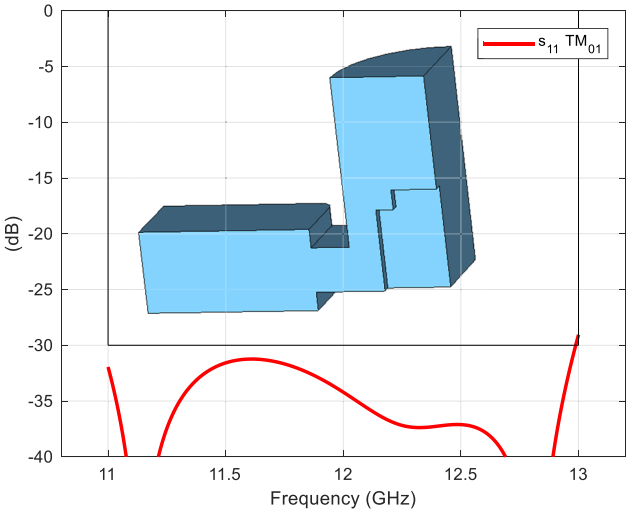


**FIGURE 3.** Return loss of the converting-section. The simulation is carried out with perfect magnetic wall (MW) boundary conditions applied at the symmetry planes of one quarter of the junction.

mode purity. In this work, we required an excitation simple and transversal to the circular waveguide axis, reducing the distance between the input common port and the 10 output ports (see Fig. 1) for achieving maximum compactness. In addition, the transversal size of the circular waveguide had to be low enough for a high mode purity. These requirements lead to the topology in [15]. For the sake of the clarity, the main points related to the mode transducer in Fig. 1 will be commented now.

The converting section (element labeled with "C" in Fig. 1 of [15]) has been replaced in this work with respect to the previous reference by a new junction with two goal in minds. On the one hand, it has been aimed to increase the return loss level up to 30 dB in the same relative bandwidth (16.7%). On the other hand, it has been also aimed to improve the purity of the excited $TM_{01}$ mode reducing the level of the undesired propagation mode (just the $TE_{11c}$ mode in this particular case and frequency band). Finally, the dimensional constrains imposed by the manufacturing have been precisely considered during the electromagnetic design.

The full-wave simulation of the converting section is carried out in a quarter of the structure with perfect magnetic wall (MW) boundary condition at its two symmetry planes. With these boundary conditions, the $TM_{01}$ is the only propagating mode in the operation band in the circular waveguide for this particular structure. The return loss, obtained very efficiently with the CST Microwave Studio [20], is shown in Fig. 3.

The feeding network is the other element of the mode transducer in Fig. 1(a). It connects the input with the two arms of the converting section. The elements labeled "A" and "B" in Fig. 1 of [15] have been resigned, changing also the connection lengths. The transducer obtained after this process, with its actual aspect ratio, is shown in the upper part of Fig. 1(a).

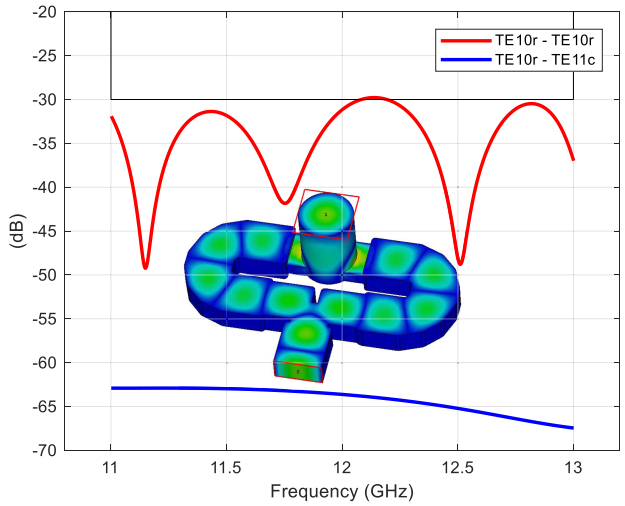


**FIGURE 4.** Simulated S-parameters of the final mode transducer (converting section with feeding network, showing the electric field configuration): Return loss for the $TE_{10r}$ rectangular mode and attenuation of the $TE_{11c}$ circular mode when it is excited by the $TE_{10r}$.

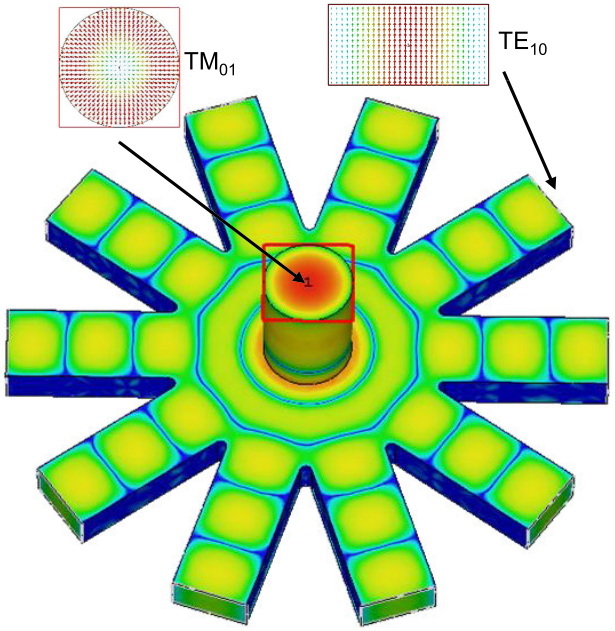


**FIGURE 5.** 3D CAD view of the proposed 10-way radial junction for the divider showing the electric field configuration. The output waveguides (WR75) are directly attached to the junction base without irises or coupling elements. The circular waveguide is excited by the $TM_{01}$ mode, not by the fundamental mode.

The next step in this design process is to cascade the converting section with the feeding network, for a final full-wave optimization of the return loss, and the level of the first undesired mode. The simulated results of the complete mode transducer are shown in Fig. 4, along with the electric field configuration in the inset of the figure. The return loss for the $TE_{10r}$ mode (the $r$ in the sub-index identifies that is a mode of the rectangular port) is better than 30 dB. The attenuation of the $TE_{11c}$ circular mode when the junction is excited by the $TE_{10r}$ rectangular mode is higher than 60 dB, guaranteeing a high purity in the mode conversion.

## III. DESIGN OF THE 10-WAY RADIAL JUNCTION EXCITED BY THE $TM_{01}$ MODE

The $TM_{01}$ mode, generated at the common circular waveguide when the transducer is excited by the rectangular port, is the input signal for the radial junction shown in Fig. 5. This $TM_{01}$ mode is equally divided into the $N = 10$ output ports. The division preserves the same magnitude and phase of the outputs at the 10 ports. The reason is the symmetry of both, the junction, and the field pattern of the $TM_{01}$ mode. Thus, the transmission parameters from the $TM_{01}$ mode to the $TE_{10}$ modes in each one of the 10 rectangular output ports will be the same, as long as the manufacturing is accurate enough.

The outputs of the junction are 10 WR75 standard rectangular waveguides, attached to the bottom of the structure in $H$-plane configuration. In this topology, there are no irises and the radius of the base is not enlarged, minimizing the losses and increasing the power handling, since no coupling windows are used. Moreover, the junction has to be matched when it is excited by the $TM_{01}$ circular waveguide mode. This has been achieved by placing a metallic element at the center of the junction. Thus, the proposed junction fulfills all the electric requisites for the power divider, but also the mechanical ones. In fact, this approach simplifies the manufacturing and reduces the cost, since the junction is split in the same body and cover configuration used in the mode transducer of Fig. 2.

This proposed junction, although it has a radial symmetry, is different to those used in dividers working in the $TE_{01}$ circular waveguide mode [9]–[13]. In these dividers, since they are using the $TE_{01}$ mode, waveguides are naturally distributed along the height-side using an $E$-plane configuration. Moreover, the $H$-plane distribution in Fig. 5 can be seen in turnstile junctions [21], [22]. However, it is emphasized here that in turnstile junctions, the number of rectangular ports is only $N = 4$ (not a generic $N$ as here, that is actually $N = 10$, making the physical arrangement much more complicate). More important, turnstile junctions are excited by the fundamental $TE_{11}$ orthogonal modes of the circular waveguide.

The matching element controlling the return loss at the circular waveguide is basically a metallic post or cylinder that preserves the radial symmetry, placed at the bottom of the junction. In this design, two stacked cylinders are necessary to cope with the specified bandwidth (see the inset in Fig. 6). Since the excitation in the circular waveguide is the $TM_{01}$ mode, MW boundary conditions are applied at the symmetry planes of one quarter of the divider in order to increase the efficiency of the computer simulations. The simulated responses are shown in Fig. 6. The return loss is better than 30 dB in the design band. The insertion loss in ports $P_1$, $P_2$ and $P_3$ is close to the theoretical value of 4.8 dB that corresponds to a 3-way divider, which here represents one quarter of the actual structure.

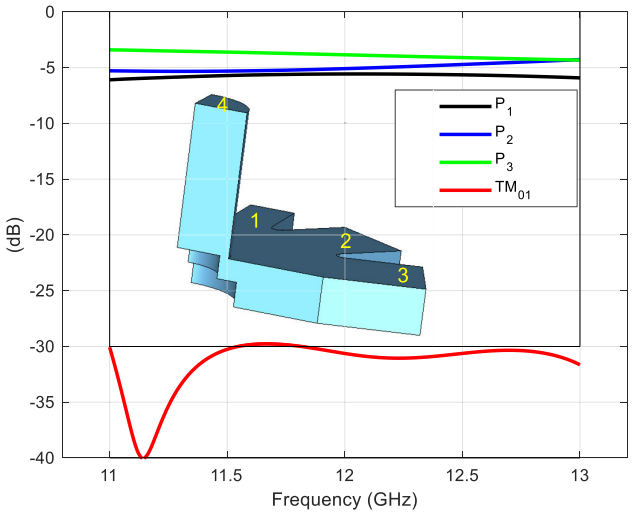


**FIGURE 6.** S-parameters of the radial junction, simulated with one quarter of the junction shown in the inset along with the port numbering. It is shown the response of the reflection coefficient of the $TM_{01}$ mode, and the transmission to the rectangular ports.

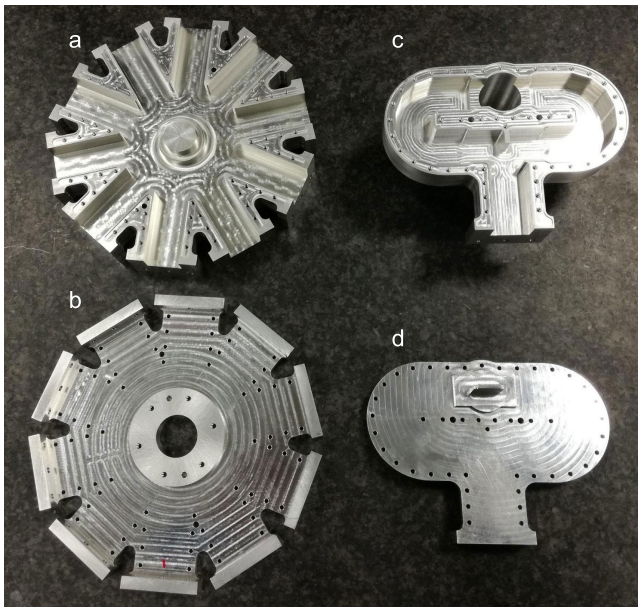


**FIGURE 7.** Four different parts forming the power divider: a) and b) body and cover of the radial junction, respectively; c) and d) body and cover of the mode transducer, respectively.

The power divider can be used in diverse areas related to high-energy, such as plasma heating, particle accelerators, etc.. Bearing in mind these applications, the estimation of the power handling has been carried out at the lowest operation frequency of 11 GHz in the most critical case. A limit of 137 kW is obtained when a breakdown field of 30 kV/cm is assumed for the air-filled device. This value has been calculated taking into account the most critical dimension of the power divider, which is found in the 10-way radial junction. As it can be observed in the inset of Fig. 6, this dimension is the distance between the last matching cylinder and the outer circular waveguide. The limit of 137 kW could be substantially increased if the power divider is filled with an insulator gas such as $SF_6$.

## IV. FINAL DESIGN OF THE POWER DIVIDER. EXPERIMENTAL RESULTS

The mode transducer and the 10-way radial junction are connected to obtain the final design of the power divider. In order to guarantee that the cascading of these two parts preserves a return loss better than 25 dB, a final full-wave optimization must be carried out. This optimization will be very fast, since the performance of each part is completely controlled in the specified bandwidth. On one hand, the return loss level for both parts in each separate design was 30 dB, *i.e.*, with a margin of 5 dB with respect to the final requirement. On the other hand, the levels of the non-desired modes in the circular waveguide connecting the two parts have been kept very low, reducing their eventual interaction. Therefore, only a few parameters are refined in the final optimization: the height of the septum in the transducer and the radius and height of the two matching cylinders in the divider (5 parameters).

The final design of the 10-way power divider has been manufactured in aluminum, using Computer Numerical Control (CNC) machining. Two parts correspond to the transducer and those other two for the radial junction. In both cases, the approach for $H$-plane circuits has been followed: it is machined a body with the main elements covered by a lid. The four parts can be seen in Fig. 7 before the assembly of the device. A photograph of the prototype already assembled in the test bench is shown in Fig. 8. It shows the experimental characterization of the scattering parameters with a Vectorial Network Analyzer (VNA) and high-precision WR75 matching loads (*i.e.*, with return loss in the calibration better than 40 dB).

The experimental results for the return loss are compared with the expected values in Fig. 9. The power divider is excited by the input rectangular waveguide (port number 11 in the 3D view of Fig. 9), and the measured return loss is better than 25 dB in the design band. It is very close to the expected response. In fact, the small differences with the theory can be explained with a sensitivity analysis taking into account the tolerances of $\pm 0.02$ mm associated to the manufacturing.

The experimental results for the transmission parameters in magnitude and phase are shown in Figs. 10 and 11, respectively. They are obtained connecting one port of the VNA to the input rectangular waveguide (see the port numbers in the inset of Fig. 9). The other port of the VNA is connected to one of the output ports (1 to 10), while the other remaining 9 ports are connected to the high-precision matching loads. The measured results for the magnitude are shown in Fig. 10. The figure also includes the reference value for an ideal case of metallic walls with perfect conductor ($\sigma = \infty$, $-10.0$ dB). It also includes the average reference value for aluminum conductivity ($\sigma_{Al} = 37.8$ MS/m, $-10.06$ dB). Since the average value of the measurements is close to $-10.12$ dB, these results show that the effective conductivity achieved in

**FIGURE 8.** Photograph of the manufactured prototype in the test bench, showing the Vectorial Network Analyzer (VNA) and the high-precision matching loads for the accurate S-parameters characterization.

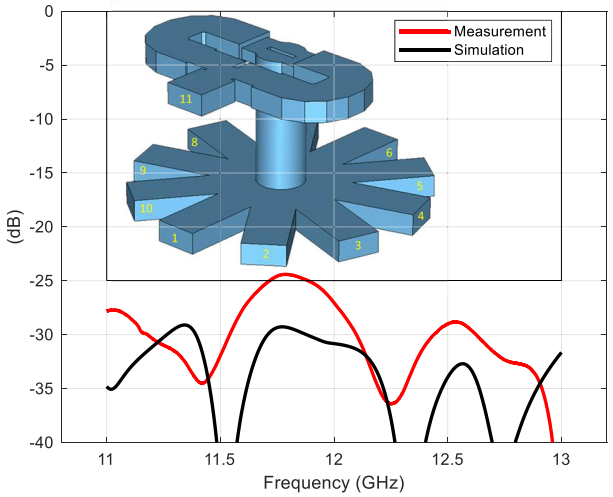


**FIGURE 9.** Comparison of the return loss between the simulation with the aluminum conductivity $\sigma_{Al} = 37.8$ MS/m and the measurement. The power divider is excited by the common input rectangular port (port number 11 according to the 3D CAD view in the inset).

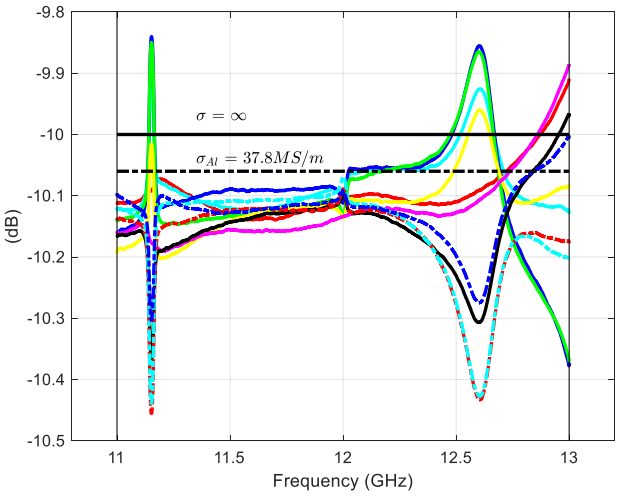


**FIGURE 10.** Experimental results: measured insertion loss of the 10-way power divider. It is included the expected simulated value for a perfect conductor $\sigma = \infty$ (−10 dB), and the expected simulated average value for aluminum conductivity $\sigma_{Al} = 37.8$ MS/m (−10.06 dB), showing a balance inside a margin of ±0.3 dB.

the prototype with the CNC manufacturing is very close to the nominal value for the aluminum.

The maximum difference between the transmission parameters is also a very important figure of merit, since it has to be as small as possible. Fig. 10 shows that the amplitude balance is inside a small margin of ±0.3 dB. This result can be explained by the surface roughness associated to the manufacturing, and, the asymmetries generated by the milling accuracy (±0.02 mm), which lead to small variations in the transmission to the different ports. Fig. 11 shows the phase of the transmission to the 10 output ports. Since these curves almost overlap, a detail of the phase difference is shown in the inset of the same figure. The difference between the phases of the transmission parameters, *i.e.*, the phase balance, is also within a small margin of ±0.45°. Thus, the balance in both magnitude and phase for the transmission parameters is very good.

The experimental results for the isolation between the rectangular output ports is shown in Fig. 12. The figure shows the measured and simulated results for the case of excitation by port number 4 (according to the port numbers in the inset of Fig. 9). This test represents one generic case of isolation, since the structure presents radial symmetry and the results exciting by other rectangular output ports are similar. When the power divider is excited by port number 4, the transmission to the adjacent ports is measured, providing the S-parameters $s_{5,4}$, $s_{6,4}$, ..., $s_{9,4}$ in the figure. The comparison with the simulated response is excellent. As it could be expected, the lowest isolation corresponds to the $s_{94}$ parameter, since it is the transmission between two opposite ports.

The $s_{44}$ parameter (the results for other output ports would be similar) is shown in Fig. 13, very close to the simulation as well. These results confirm the accurate machining, and they support the proposed design approach, where the manufacturing constrains are incorporated into the design of the parts from the very beginning. It is highlighted that the $s_{44}$ parameter is obtained when all the other ports are terminated in matched loads. However, for actual power combination, all the ports 1 to 10 are excited in-phase. For power division,

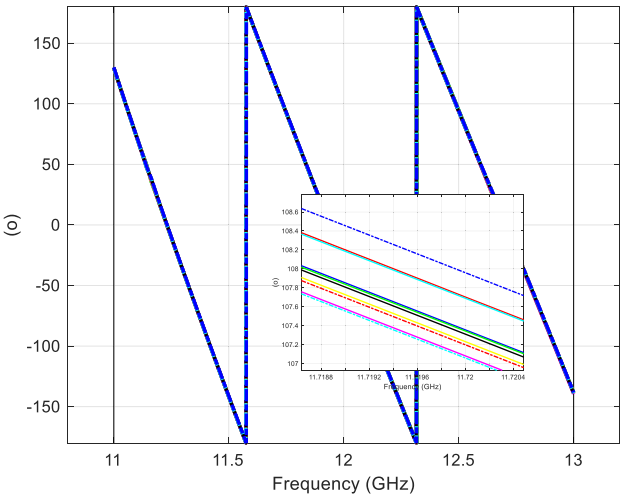


**FIGURE 11.** Experimental results: measured phase (in degrees) of the transmission parameters for the 10-way power divider (a detail is shown in the inset of the figure), showing a balance inside a margin of ±0.45°.

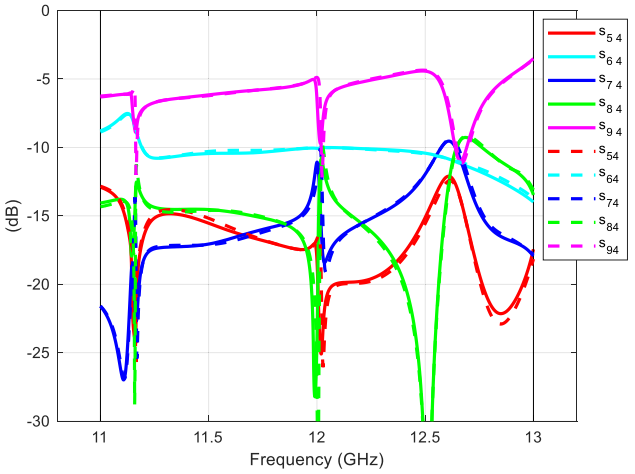


**FIGURE 12.** Experimental results: measured isolation (continuous line) when the power divider is excited by port number 4 (see the inset in Fig. 9), measuring the transmission to the adjacent ports for obtaining the $s_{54}, \ldots, s_{94}$ parameters. The measured values are compared with the simulated values (dashed line) using the aluminum conductivity for the metallic walls $\sigma_{Al} = 37.8$ MS/m.

the junction is excited by port 11. In both cases of combination/division, the return loss for these two modes of operation is represented in Fig. 9. Moreover, the peaks in Figs. 12 and 13 at approximately 11.2, 12.0 and 12.6 GHz are found when the junction is excited asymmetrically (only by port 4 in this example) out of these two modes of operation. The manufacturing asymmetries also lead to differences in the transmission parameters, although within a small margin of ±0.3 dB yielding a great overall performance summarized in the efficiency parameter.

The combining efficiency parameter [23] has been characterized to have an overall figure of merit for the power divider. This parameter takes into account the combination of the transmission from the input to all the output ports in

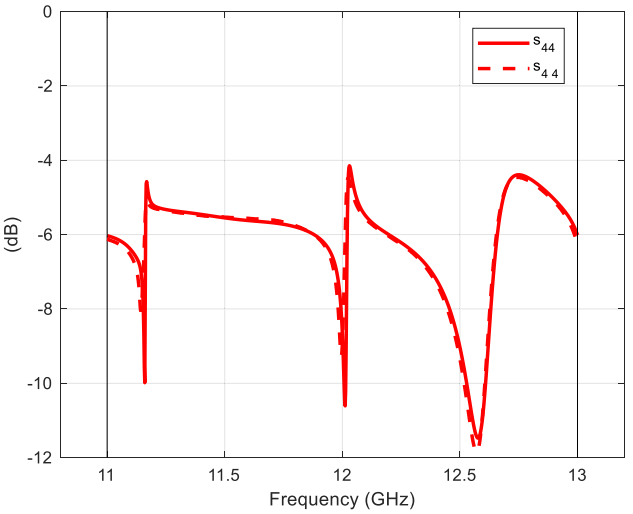


**FIGURE 13.** Experimental results: measured $s_{44}$ parameter (continuous line) when the power divider is excited by port number 4 (see the inset in Fig. 9) and all the other ports are terminated in their matched load. Measurement is compared with the simulated value (dashed line) using the aluminum conductivity for the metallic walls $\sigma_{Al} = 37.8$ MS/m.

both magnitude and phase. It is computed as

$$\xi = \frac{1}{10}\left|\sum_{k=1}^{10} s_{k,11}\right|^2, \tag{1}$$

where the port numbering is shown in the inset of Fig. 9.

The expected theoretical efficiency has been obtained by a full-wave analysis of the power divider taking into account the aluminum conductivity $\sigma_{Al} = 37.8$ MS/m in all the metallic walls. The experimental efficiency has been obtained with the measured transmission parameters, and it is better than 96.5% in the design bandwidth. Fig. 14 shows the comparison between both results. It must be emphasized that the surface roughness and the milling accuracy have only reduced the theoretical efficiency a 2%, which can be associated to an excellent manufacturing.

As a summary, Table 1 compares the performance of two waveguide radial power combiners with the same center frequency and bandwidth at Ku-band. Both designs include a mode transducer from the $TE_{10}$ mode in the rectangular waveguide to a high-order mode of the circular waveguide: the $TE_{01}$ for the first case and the $TM_{01}$ for the second case. The physical parameters under comparison are the number of ways $N$, the material and the manufacturing process. The electrical parameters included in the table are the ohmic (in excess) insertion loss per way, the power handling, the amplitude and phase balance, and the power combination efficiency.

It is well known the low-loss behavior of the $TE_{01}$ circular waveguide mode. Nevertheless, the similar combination efficiencies and insertion losses of the two designs in the Table, suggest that there is not a clear prevalence of the solution based on the $TE_{01}$ (*a priori* the preferred approach) with respect to the $TM_{01}$. Although this comparison has to take

**TABLE 1. Performance comparison between two Ku-band power dividers based on the $TE_{01}$ and $TM_{01}$ circular waveguide modes, respectively.**

| Circ. Wg. Mode | $F_{cen}$ (GHz) | BW (GHz) | $N$-way Ports | Material $\sigma_{nom}$ (MS/m) | Ohmic Ins. Loss (dB) | Power Hand. (kW) | Amplitude Bal. (dB) | Phase Bal. (°) | Manufacturing and Topology | Efficiency (%) |
|---|---|---|---|---|---|---|---|---|---|---|
| $TE_{01}$ [9] | 12 | 2 | 16 WR75 | Brass 15.9 | 0.1 | 240 | ±0.15 | ±2.5 | CNC milling $E$-plane | 95 |
| $TM_{01}$ This work | 12 | 2 | 10 WR75 | Al 37.8 | 0.1 | 137 | ±0.3 | ±0.45 | CNC milling-EDM $H$-plane | 96.5 |

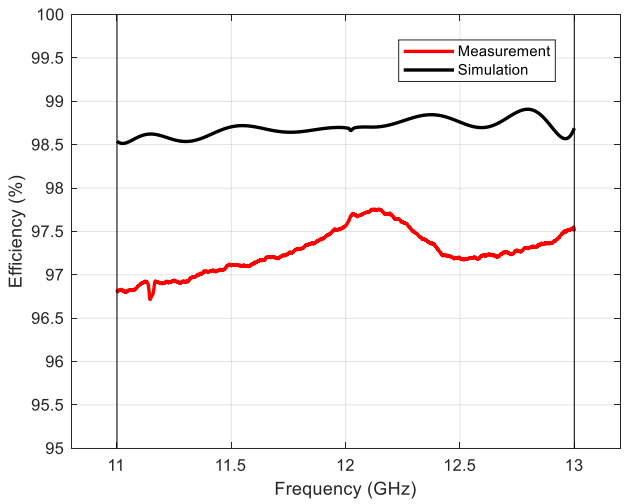


**FIGURE 14. Comparison of the combining efficiency parameter between the extracted value from the experimental results and the simulation with the aluminum conductivity $\sigma_{Al} = 37.8$ MS/m.**

into account that the materials of both designs are different (lower conductivity for the $TE_{01}$ case), there are several aspects to consider where each solution has its own pros and cons. For instance, the $TE_{01}$ approach is the best option in this case for the power handling capability according to the Table. In any case, both estimated values, 240 and 137 kW, respectively, are enough for a great variety of applications, where typically the thermal aspects become the real limiting factors.

Another key aspect in the comparison is the manufacturing. The $H$-plane configuration with the $TM_{01}$ mode has a lower cost since the body/lid structure shown in Fig.7 can be manufactured by CNC milling. However, in the case of the $TE_{01}$ mode, the more expensive Electrical Discharge Machining (EDM) technology was also necessary. In size, for a large number of ports, the $E$-plane configuration allows a more compact distribution of the ports than the $H$-plane (output rectangular waveguides arranged along the height rather than the width), although in the $H$-plane approach all the ports are polarized in the same direction.

The high purity required for the mode exciting the $N$-way radial junction can be only achieved with a careful control of the attenuation levels of the non-desired modes in the circular waveguide. In this case, the combiner based on the $TM_{01}$ mode has an intrinsic advantage: there is only one mode to control, the $TE_{11c}$. However, for the $TE_{01}$ approach, there are four propagating modes whose attenuation level must be controlled: the $TE_{11c}$, $TE_{21c}$, $TM_{11s}$ and $TE_{31c}$.

The designer has to take into account all the previous considerations to make the final selection between both circular waveguide modes. However, taking into account all the considered figures of merit, we have shown the potential of the combiner based on the $TM_{01}$ mode. It is a feasible option, not as extended as the $TE_{01}$ approach in the technical literature, but with a similar performance whose advantages can be exploited in many applications.

## V. CONCLUSION

A novel 10-way Ku-band radial power divider based on the $TM_{01}$ circular mode has been presented. The components of the power divider have been discussed, especially the main steps in the design and the manufacturing. The proposed structure exploits the symmetries of the field pattern of the $TM_{01}$ mode, generated with a mode transducer, with a very simple radial junction that allows to allocate a large number (10) of output rectangular ports in $H$-plane configuration. This also simplifies the manufacturing (key point to obtain a great performance), since both, the transducer and the divider, can be segmented in a simple configuration of a main body and a cover. Since milling can be used to fabricate the four parts, the cost is dramatically reduced.

Finally, the experimental results show a great performance in different figures of merit over the whole 16.7% fractional bandwidth (11-13 GHz) of the design: return loss better than 25 dB, difference between the transmission parameters in magnitude within ±0.3 dB and phase within ±0.45°, and efficiency higher than 96.5%. Therefore, the presented power divider based on the $TM_{01}$ mode can be a feasible alternative to the more extended approach based on the $TE_{01}$ mode.

## REFERENCES

[1] J. X. Qiu, B. Levush, J. Pasour, A. Katz, C. M. Armstrong, D. R. Whaley, J. Tucek, K. Kreischer, and D. Gallagher, "Vacuum tube amplifiers," *IEEE Microw. Mag.*, vol. 10, no. 7, pp. 38–51, Dec. 2009.

[2] K. Kanto, A. Satomi, Y. Asahi, Y. Kashiwabara, K. Matsushita, and K. Takagi, "An X-band 250 W solid-state power amplifier using GaN power HEMTs," in *Proc. IEEE Radio Wireless Symp.*, Jan. 2008, pp. 77–80.

[3] K. J. Russell, "Microwave power combining techniques," *IEEE Trans. Microw. Theory Techn.*, vol. 27, no. 5, pp. 472–478, May 1979.

[4] K. Chang and C. Sun, "Millimeter-wave power-combining techniques," *IEEE Trans. Microw. Theory Techn.*, vol. 31, no. 2, pp. 91–107, Feb. 1983.

[5] Q. Xue, K. Song, and C. H. Chan, "China: Power combiners/dividers," *IEEE Microw. Mag.*, vol. 12, no. 3, pp. 96–106, May 2011.

[6] K. R. Vaden and R. N. Simons, "Computer aided design of Ka-band waveguide power combining architectures for interplanetary spacecraft," in *Proc. IEEE Antennas Propag. Soc. Int. Symp.*, Jul. 2005, pp. 1–7.

[7] A. E. Fathy, S.-W. Lee, and D. Kalokitis, "A simplified design approach for radial power combiners," *IEEE Trans. Microw. Theory Techn.*, vol. 54, no. 1, pp. 247–255, Jan. 2006.

[8] F. K. Gharekand, "Design of a 16 way radial microwave power divider/combiner with rectangular waveguide output and coaxial inputs," *Int. J. Electron. Commun.*, vol. 68, no. 5, pp. 422–428, May 2014.
[9] J. R. Montejo-Garai, I. Saracho-Pantoja, J. A. Ruiz-Cruz, and J. M. Rebollar, "High-performance 16-way Ku-band radial power combiner based on the $TE_{01}$-circular waveguide mode editors-pick," *Rev. Sci. Instrum.*, vol. 89, Mar. 2018, Art. no. 034703.
[10] J. R. Montejo-Garai, J. A. Ruiz-Cruz, and J. M. Rebollar, "5-way radial power combiner at W-band by stacked waveguide micromachining," *Nucl. Instrum. Methods Phys. Res. A, Accel. Spectrom. Detect. Assoc. Equip.*, vol. 905, pp. 91–95, Oct. 2018.
[11] T.-I. Hsu and M. D. Simonutti, "A wideband 60 GHz 16-way power divider/combiner network," in *IEEE MTT-S Int. Microw. Symp. Dig.*, May/Jun. 1984, pp. 175–177.
[12] M. Chen, " A 19-way isolated power divider via the $TE_{01}$ circular waveguide mode transition," in *IEEE MTT-S Int. Microw. Symp. Dig.*, Jun. 1986, pp. 511–513.
[13] L. Epp, P. Khan, and A. Silva, "Ka-band wide-bandgap solid-state power amplifier: Hardware validation," IPN Prog. Rep. 42-163, 2005.
[14] H. Matsumura and H. Mizuno, "Design of microwave combiner with waveguide ports," *Electron. Commun. Jpn.*, vol. 71, no. 8, pp. 1279–1285, 1988.
[15] J. R. Montejo-Garai, J. A. Ruiz-Cruz, and J. M. Rebollar, "Design of a ku-band high-purity transducer for the $TM_{01}$ circular waveguide mode by means of t-type junctions," *IEEE Access*, vol. 7, pp. 450–456, 2019. doi: 10.1109/ACCESS.2018.2885489.
[16] G. L. Ragan, *Microwave Transmission Circuits* (MIT Radiation Laboratory), vol. 9. New York, NY, USA: McGraw-Hill, 1948.
[17] A. Tribak, J. Zbitou, A. M. Sanchez, and N. A. Touhami, "Ultra-broadband high efficiency mode converter," *Prog. Electromagn. Res. C*, vol. 36, pp. 145–158, 2013. doi: 10.2528/PIERC12111905.
[18] X.-M. Li, J.-Q. Zhang, X.-Q. Li, and Q.-X. Liu, "A high-power orthogonal over-mode circular waveguide $TE_{11}$-$TM_{01}$ mode converter," *IEEE Microw. Wireless Compon. Lett.*, vol. 27, no. 12, pp. 1095–1097, Dec. 2017.
[19] A. Cui, G. Wang, T. Jiang, H. Shao, J. Sun, X. Wu, X. Bai, X. Zhang, and Z. Zhang, "High-efficiency, broadband converter from a rectangular waveguide $TE_{10}$ mode to a circular waveguide $TM_{01}$ mode for overmoded device measurement," *IEEE Access*, vol. 6, pp. 14996–15003, 2018. doi: 10.1109/ACCESS.2018.2815530.
[20] *Computer Simulation Technology*. Accessed: Jul. 14, 2019. [Online]. Available: https://www.cst.com/
[21] C. Montgomery, R. Dicke, and E. Purcell, *Principles of Microwave Circuits*. London, U.K.: Electromagnetic Waves, 1987.
[22] J. A. Ruiz-Cruz, J. R. Montejo-Garai, C. A. Leal-Sevillano, and J. M. Rebollar, "Orthomode transducers with folded double-symmetry junctions for broadband and compact antenna feeds," *IEEE Trans. Antennas Propag.*, vol. 66, no. 3, pp. 1160–1168, Mar. 2018.
[23] M. S. Gupta, "Power combining efficiency and its optimisation," *Proc. Inst. Elect. Eng. Microw., Antennas Propag.*, vol. 139, no. 3, pp. 233–238, Jun. 1992.

**JOSÉ R. MONTEJO-GARAI** was born in Vitoria-Gasteiz, Spain, in 1965. He received the Ingeniero de Telecomunicación degree and the Ph.D. degree from the Universidad Politécnica de Madrid, Madrid, Spain, in 1990 and 1994, respectively. Since 1989, he has been with the Grupo de Electromagnetismo Aplicado y Microondas, Universidad Politécnica de Madrid, as an Assistant Professor, until 1996 and as an Associate Professor, until 2017, where he is currently a Full Professor. His current research interests include the analysis and characterization of wave-guide structures, advanced synthesis theory and computer aided design for microwave and millimeter-wave passive devices: filters, multiplexers, orthomode transducers, and beam forming networks. He has designed a plenty of passive microwave devices for communication satellites.

**JORGE A. RUIZ-CRUZ** (SM'11) received the Ingeniero de Telecomunicación degree and the Ph.D. degree from the Universidad Politécnica de Madrid, Madrid, Spain, in 1999 and 2005, respectively. Since 2006, he has been with the Universidad Autónoma de Madrid, Madrid, where he became an Associate Professor, in 2009. His current research interests include the computer-aided design of microwave passive devices and circuits (filters, multiplexers, and orthomodes).

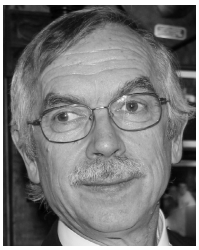

**JESÚS M. REBOLLAR** (M'15) was born in Beasain, Spain, in 1953. He received the Ingeniero de Telecomunicación degree and the Doctor degree from the Universidad Politécnica de Madrid, Madrid, Spain, in 1975 and 1980, respectively. Since 1976, he has been with the Grupo de Electromagnetismo Aplicado y Microondas, Universidad Politécnica de Madrid, as an Assistant Professor, until 1982 and an Associate Professor, until 1988, where he was appointed to Professor of teoría electromagnética. His current research interests include electromagnetic wave propagation in waveguide structures, interactions of electromagnetic fields with biological tissues, and particularly computer-aided design for microwave and millimeter-wave passive devices: filters, multiplexers, polarizers, orthomode transducers, and beam forming networks. He has designed many of the above components for communication systems on board satellites.